Electronic Supplementary Material (ESI) for ChemComm.

Supporting Information

Aryl-Viologen Pentapeptide Self-Assembled Conductive Nanofibers

David E. Clarke,[†‡] Magdalena Olesinska,[†‡] Tobias Mönch,[†] Ben Schoenaers,[§] Andre Stesmans,[§] and Oren A. Scherman[†*]

[†] Melville Laboratory for Polymer Synthesis, Department of Chemistry, University of Cambridge, CB2 1EW, UK

[§] Department of Physics and Astronomy, KU Leuven, Celestijnenlaan 200D, 3001 Leuven, Belgium

[‡] These authors contributed equally

Experimental

Materials

All Fmoc-protected amino acids, solvents and rink amide 4-methyl-benzhydrylamine (MBHA) resin used for peptide synthesis were purchased from AGTC Bioproducts (UK). All other solvents and reagents were purchased from Sigma-Aldrich (UK) and used as received: 4,4′-Bipyridine (CAS: 553-26-4), 1-chloro-2,4-dinitrobenzene (≥99%, CAS: 97-00-7), 4-(4-Aminophenyl)butyric acid (≥95%, CAS: 15118-60-2), Methyl iodide (≥99.0%, CAS: 74-88-4).

Synthesis of 1-(2,4-dinitrophenyl)-[4,4'-bipyridin]-1-ium

4,4′-Bipyridine (10g, 64 mmol) and 1-chloro-2,4-dinitrobenzene (13 g, 64 mmol) were refluxed in ethanol (250 mL) for 24 hr under the protection of N_2 gas. After cooling to room temperature, the mixture was concentrated to ca. 30 mL and precipitated by adding diethyl ether (600 mL). After standing for 1 hr, the precipitate was collected by suction filtration and washed with diethyl ether. After being dried in a vacuum-oven at 60 °C, a yellow solid of (mg) was obtained in 80% yield. ^{1}H NMR (400 MHz, D_2O) δ (ppm): 9.33 (d, *J* = 2.4 Hz, 1H), 9.18 (d, *J* = 6.5 Hz, 2H), 8.91-8.86 (m, 1H), 8.77 (d, *J* = 5.7 Hz, 2H), 8.61 (d, J = 6.5 Hz, 2H), 8.20 (d, J = 8.7 Hz, 1H)., 8.00-7.93 (m, 2H). ESI-MS: *m/z* $[M]^+$ calcd for $C_{16}H_{11}N_4O_4$: 323.0775, found: 323.0775

Synthesis of 1-(4-(4-carboxybutyl)phenyl)-1'-methyl-[4,4'-bipyridine]-1,1'-diium (2 steps)

1-(2,4-dinitrophenyl)-[4,4'-bipyridin]-1-ium (2 g, 5.57 mmol), 4-(4-Aminophenyl)butyric acid (3 g, 16.72 mmol) and catalytic amount of trimethylamine were refluxed in ethanol (250 mL) overnight under the protection of N_2 gas. After cooling to room temperature, the mixture was concentrated to ca. 30 mL and precipitated by adding diethyl ether (600 mL). After standing for 1 hr, the precipitate was collected by suction filtration and washed with diethyl ether. Obtained 1-(4-(3-carboxypropyl)phenyl)-[4,4'-bipyridin]-1-ium (1 g, 2.81 mmol) and methyl iodide (396 mg, 174 µl, 2.81mmol) were refluxed in ethanol (100 mL) overnight under the protection of N_2 gas. After cooling to room temperature, the mixture was concentrated to ca. 30 mL and precipitated by adding diethyl ether, the precipitate was collected by suction filtration and washed with diethyl ether. After being dried in a vacuum-oven at 60 °C, a brown solid of 1-(4-(4-carboxybutyl)phenyl)-1'-methyl-[4,4'-bipyridine]-1,1'-diium (700 mg) was obtained in 49.8% yield. ^{1}H NMR (500 MHz, D_2O) δ (ppm): 9.31-9.24 (m, 2H), 9.01 (d, *J* = 6.6 Hz, 2H), 8.66-8.59 (m, 2H), 8.52 (d, *J* = 6.6 Hz, 2H), 7.70-7.62 (m, 2H), 7.55 (d, *J* = 8.6 Hz, 2H), 4.45 (s, 3H), 2.77 (t, *J* = 7.5 Hz, 2H), 2.34 (t, *J* = 7.3 Hz, 2H), 1.94 (p, *J* = 7.5 Hz, 2H). ^{13}C NMR (125 MHz, D_2O) δ (ppm): 150.49, 149.63, 146.33, 145.25, 140.30, 130.65, 126.86, 126.72, 123.90, 48.36, 33.91, 33.50, 25.81. ESI-MS: *m/z* $[M\text{-}2Cl]^{2+}$ calcd for $C_{21}H_{22}N_2O_2$: 167.0835, found: 167.0833

Synthesis and Characterisation of I3D2 Peptide and AVI3D2 Conjugate

An initial batch of the I3D2 peptide sequence was synthesized using solid-phase methodology (FMOC, tBu, MBHA resin) on an automated microwave peptide synthesizer (Liberty, CEM). Following the automated synthesis, a manual coupling step was used to fabricate the AVI3D2 conjugate material. 0.25 mmol of I3D2 labelled resin was reacted with 2 equivalence of the synthesized AV, along with 2.5 equivalence of both HCTU and DIPEA in DMF and shaken overnight. Both the crude I3D2 peptide and AVI3D2 conjugate were cleaved from

the resin with a cleavage cocktail of 95% trifluoroacetic acid (TFA), 2.5% triisopropyl silane and 2.5% DI H_2O and left to shake for 2.5 hours. Following cleavage, the crude peptides were precipitated and washed with cold diethyl ether (DEE), then left to dry under vacuum overnight.

The crude peptides were then purified by high pressure liquid chromatography (HPLC) using a Phenomenex C18 Kinetic-Evo column with a 5 µm pore size, a 110 Å particle size and with the dimensions 150 x 21.2 mm. A gradient from 5% acetonitrile 95% water to 100% acetonitrile was run, the I3D2 peptide was purified in basic conditions (0.1% ammonium hydroxide and 20 mM ammonium formate) and the AVI3D2 conjugate material in acidic conditions (0.1% TFA). Following purification, the peptide and AVI3D2 conjugate identities were verified by a combination of analytical HPLC (Figure S1), fourier-transform mass spectrometry (FTMS) courtesy of National Mass Spectrometry Service, Swansea UK (Figures S3 and S4) and ^{1}H-NMR (Figures S9 and S10).

Nuclear Magnetic Resonance Spectroscopy (NMR)

^{1}H-NMR, ^{13}C-NMR, DOSY, COSY and NOESY spectra were acquired in D_2O, D_2O doped with K_2CO_3 (I3D2 peptide) or D_2O/DCl (NOESY, pD 4.0) at 298 K. Spectra were recorded on a Bruker AVANCE III HD with TCI Cryoprobe system (500 MHz) being controlled by TopSpin2. Pre-saturation of the residual solvent signal was utilized for the 1H-NMR. In addition, the NOESY experiments were carried out using a standard pulse sequence 'noesygpphpp' with 2 s relaxation delay and 1000 ms mixing time.

UV/Vis Spectrometry

UV/Vis spectra for AVI3D2 and AV (0.1 mM) at both pH 4 and pH 8 were recorded using a Varian Cary 4000 UV/Vis spectrophotometer using a cuvette with 1 cm path length at 298 K.

Fluorescence Spectrometry

The fluorescence of the AVI3D2 conjugate was recorded using steady state photoluminescence emission spectra at room temperature with a Varian Cary Eclipse Flourimeter. Solutions were prepared at both 1 mM (pH 4 & 8) and 8 mM (pH 4 & 8), and the spectra recorded using a 120 µL quartz three-window fluorescence cuvette. Samples were excited at 320 nm with a 5 nm excitation/emission slit.

Circular Dichroism

Circular Dichroism (CD) measurements were carried out in the far-UV on a Chirascan spectrometer (Applied Photophysics). All scans were performed at 298 K from 180-260 nm at 0.5 nm intervals with an acquisition time of 1 second and using a 0.1mm path length quartz plate cuvette. The spectra collected was averaged across two scans and corrected via background subtraction.

Fourier Transform Infrared Spectroscopy

To further probe the formation and nature of the β-sheet structures, Fourier transform infrared spectroscopy (FT-IR) was carried out using a Perkin-Elmer Spectrum 100 FT-IR Spectrometer in the amide I region (1550 - 1700 cm^{-1}) at a resolution of 1 cm^{-1} and averaged from 16 consecutive scans. The solutions were lyophilized, and the

resultant dried material used for analysis. All the spectra were normalized to the absorbance at 1550 cm^{-1}, which is assumed to be insensitive to peptide secondary structure.

Conductive Atomic Force Microscopy

Conductive Atomic Force Microscopy (c-AFM) was utilised to investigate the morphology and conductive properties of the different materials. All samples were prepared by pipetting 5 μl of a stock solution onto a gold substrate and spread using a N_2 jet to obtain a thin layer. They were then left to dry overnight under vacuum. All measurements were carried out on a MFP-3D AFM System (Asylum/Oxford Instruments) operating in contact mode coupled with an ORCA™ module and a PtIr coated SCM-PIC tip (Bruker) with nominal spring constant of 0.2 N/m. Images were produced using a gain of 5 x 10^8 volts/amp and a -4.0 V bias. The system's NPS™ nano-positioning closed loop sensors and "pick a point" force curve interface was used to positioned the cantilever at a point of interest on the map. The bias voltage was then swept from -10.0 to 10.0 V and the response current measured. The conductivity (IV) data was averaged across 4 scans.

Electron Spin Resonance Spectroscopy

Electron Spin Resonance (ESR) spectra were obtained using a JEOL JES-FA100 (X-band, ~ 9.43 GHz) spectrometer with the samples being continuously irradiated by a mercury-based UV light source. Conventional continuous wave absorption first derivative measurements were carried out with periodic modulation $B_m\cos(\omega_m t)$ of the applied magnetic field **B**. The accurate determination of g values and spin concentrations was aided by making use of a co-mounted calibrated Mn^{2+} marker sample. All the ESR measurements were carried out at room temperature using incident microwave power P_μ = 2 mW and modulation of the applied magnetic field with amplitude B_m = 0.05 mT, modulation frequency $\omega_m/2\pi$ = 100 kHz, and time constant τ = 0.03 s. A field sweep of 100 G is performed in 30 s. The small signals emerging in the spectra at g = 2.0138 ± 0.0002 and g = 2.0006 ± 0.0001 originate from the cavity background and quartz sample holder (more specifically the E'_γ defect [1]), respectively.

Supplementary Figures

HPLC

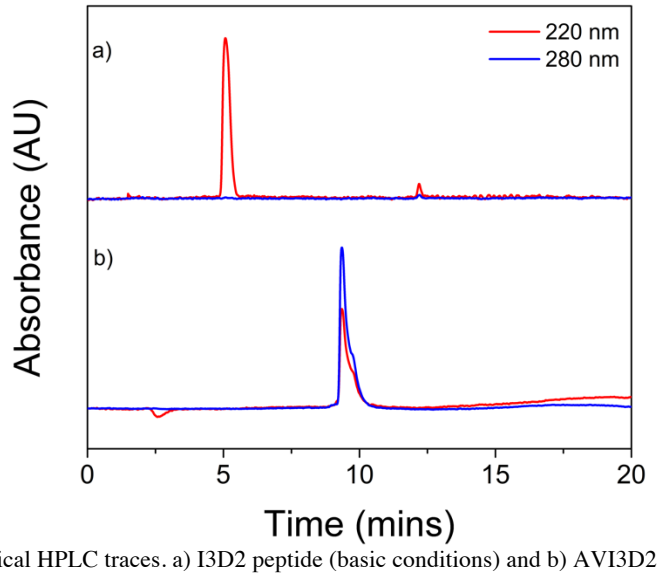

Figure S1. Analytical HPLC traces. a) I3D2 peptide (basic conditions) and b) AVI3D2 conjugate (acidic conditions).

Mass Spectrometry

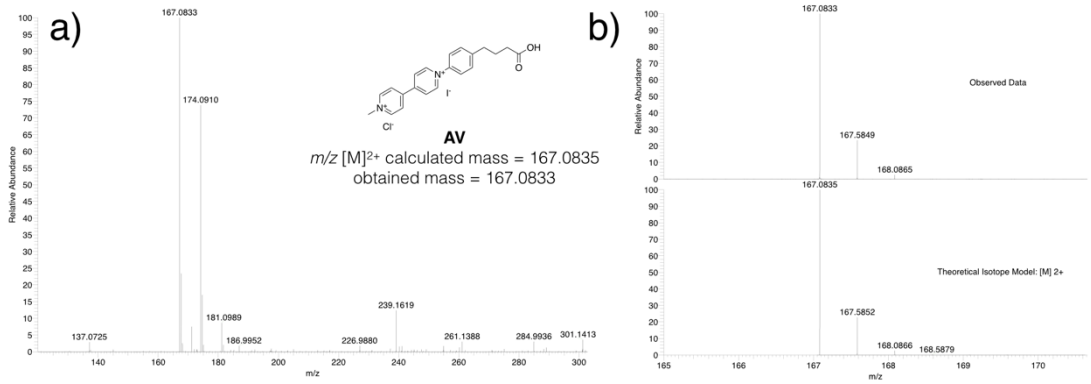

Figure S2. a) Positive ion FTMS and b) accurate mass FTMS of AV, performed in MeOH (courtesy of the National Mass Spectrometry Service, Swansea, UK).

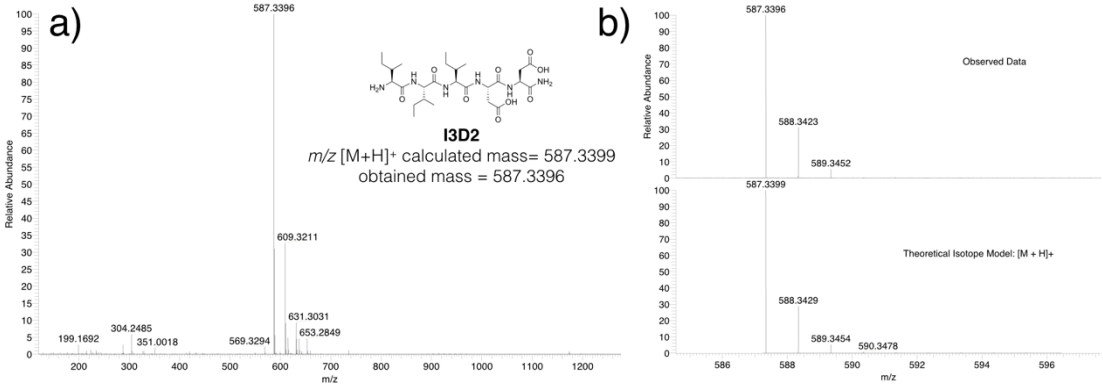

Figure S3. a) Positive ion FTMS and b) accurate mass FTMS of I3D2, performed in a mixture of MeOH/NH_4OAc (courtesy of the National Mass Spectrometry Service, Swansea, UK).

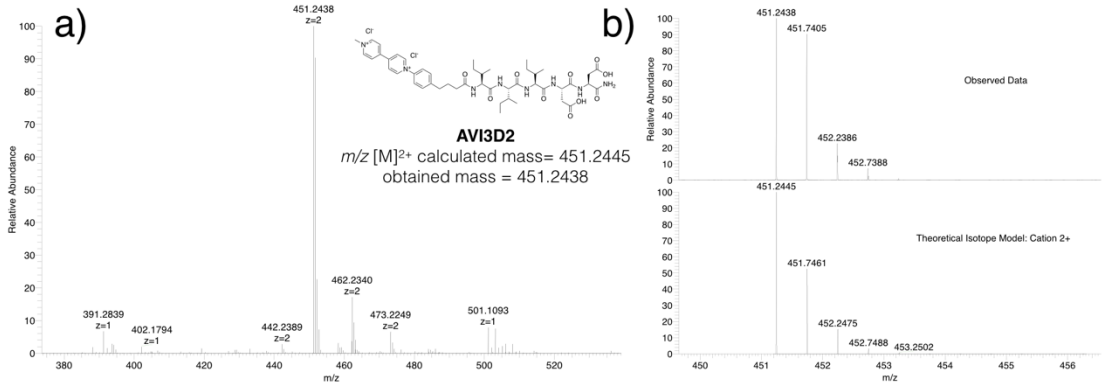

Figure S4. a) Positive ion FTMS and b) accurate mass FTMS of AVI3D2, performed in a mixture of MeOH/NH_4OAc (courtesy of the National Mass Spectrometry Service, Swansea, UK).

NMR Studies - AV

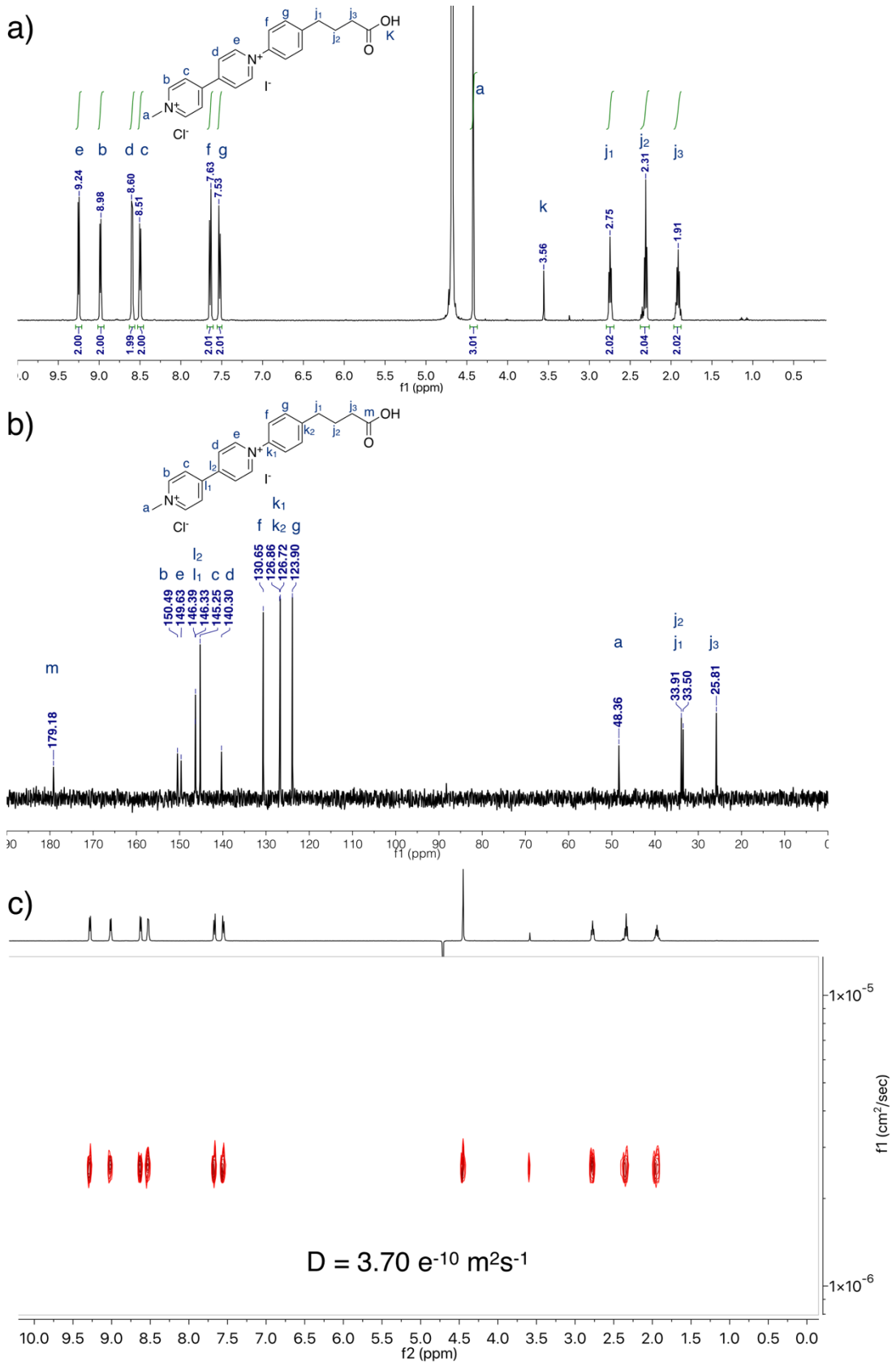

Figure S5. a) ^{1}H-NMR, b) ^{13}C-NMR, and c) DOSY spectra of AV (500 MHz, D_2O).

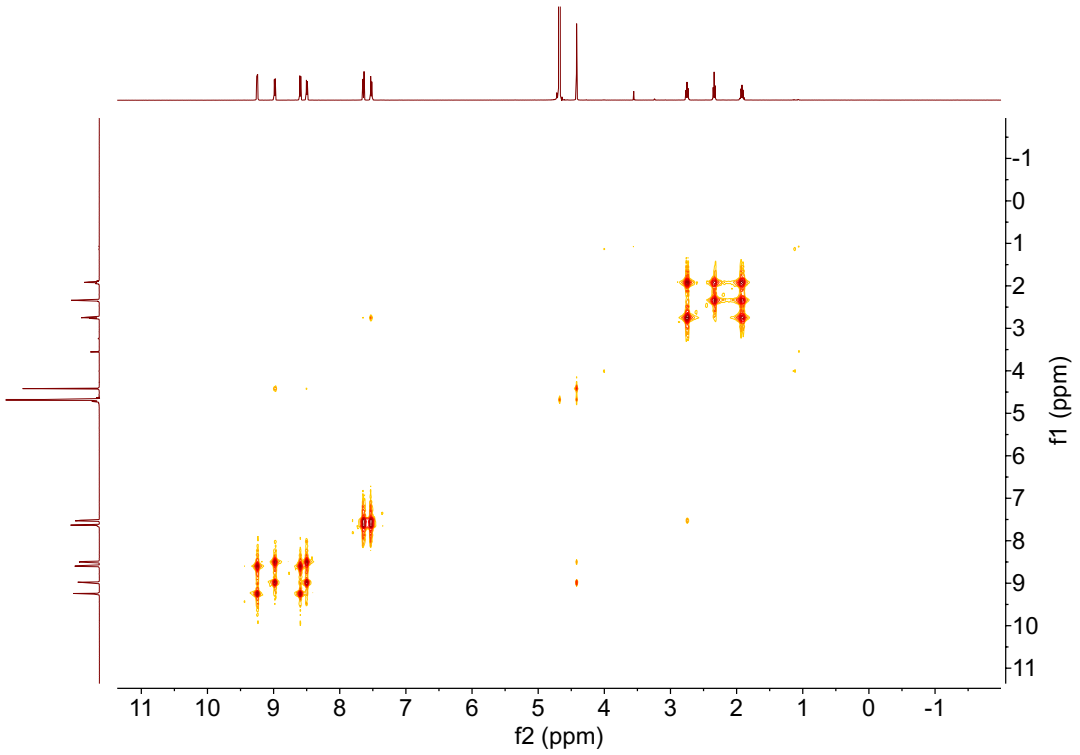

Figure S6. COSY spectra of AV (500 MHz, D_2O).

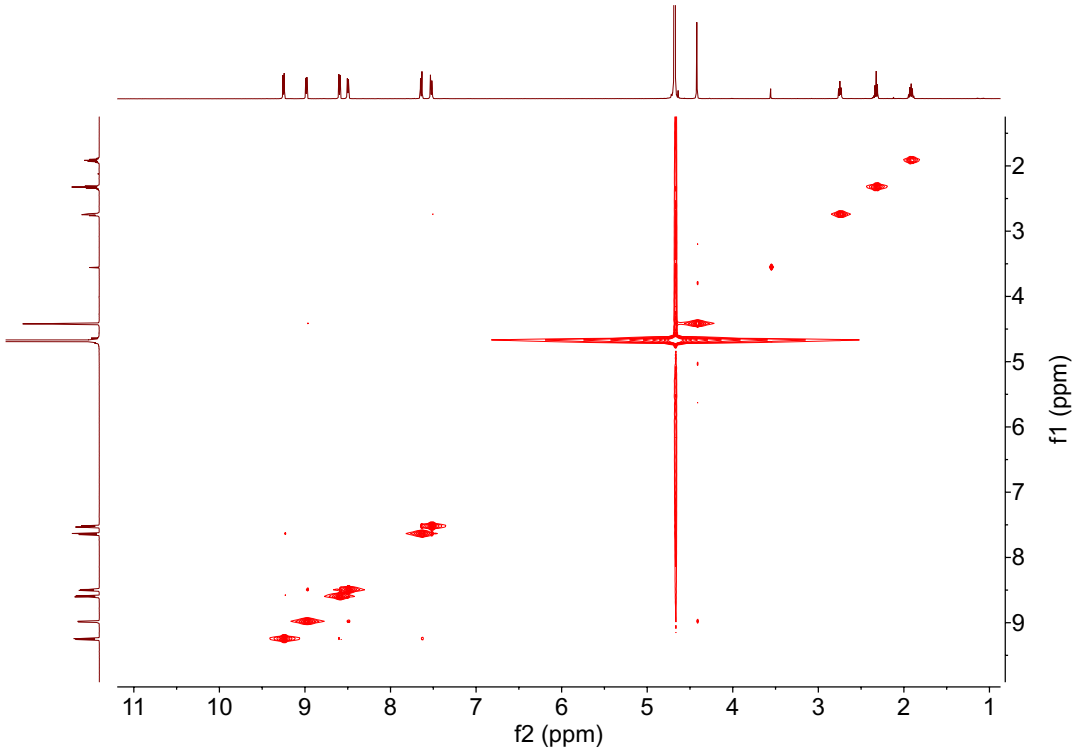

Figure S7. NOESY spectra of AV, pD 7.40 (500 MHz, D_2O).

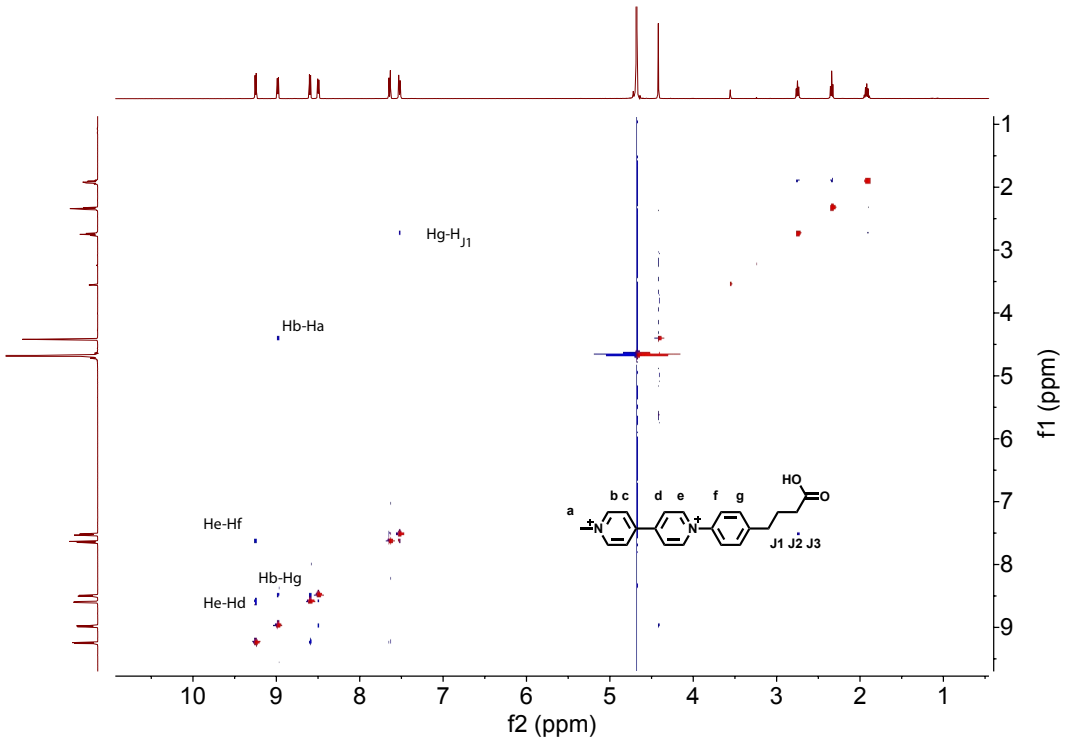

Figure S8.NOESY spectra of AV in pD 4.0 (500 MHz, D_2O/DCl).

NMR Studies – I3D2 Peptide

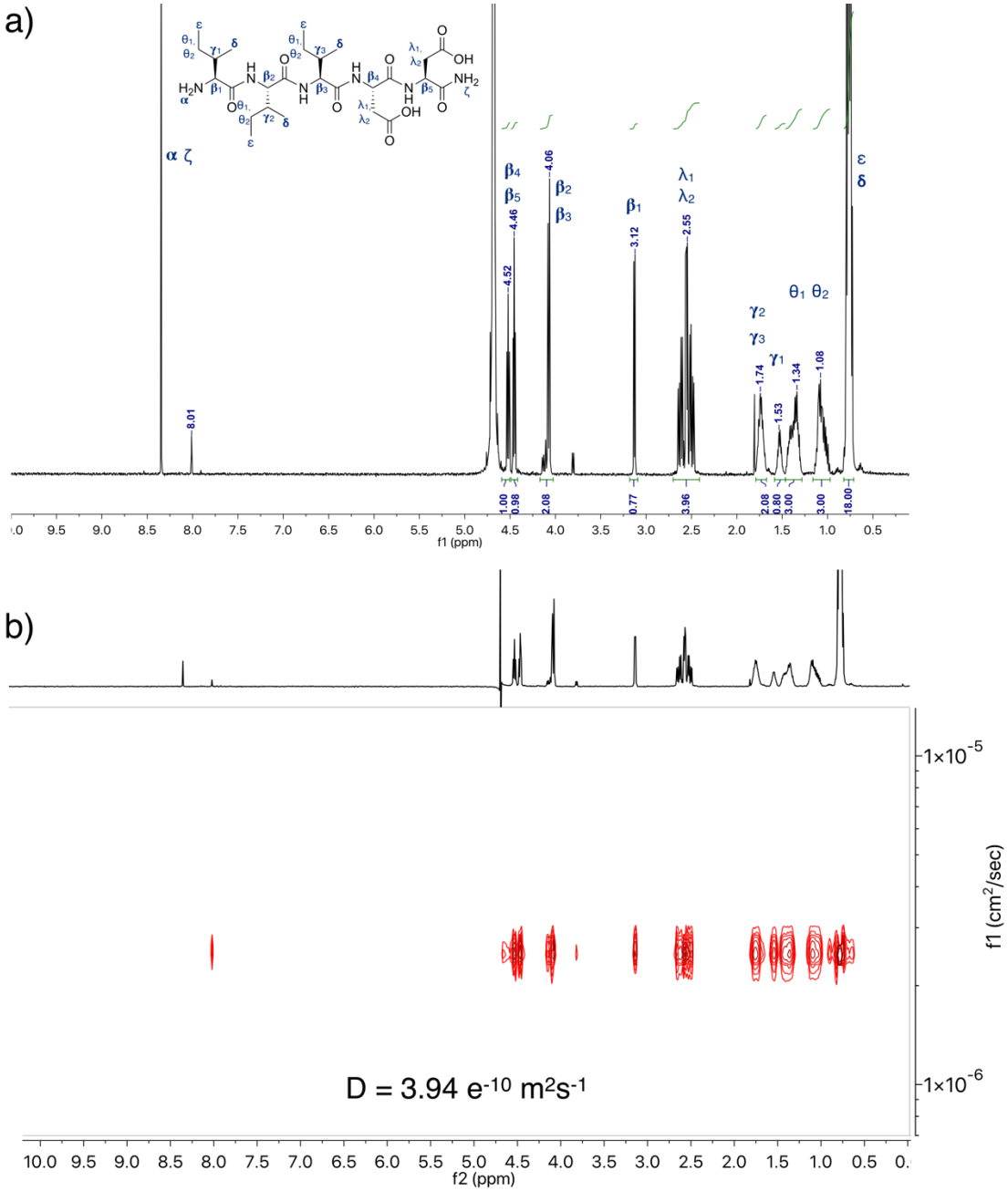

Figure S9. a) ^{1}H-NMR and b) DOSY spectra of I3D2 peptide (500 MHz, D_2O/ K_2CO_3).

NMR Studies – AVI3D2 Conjugate

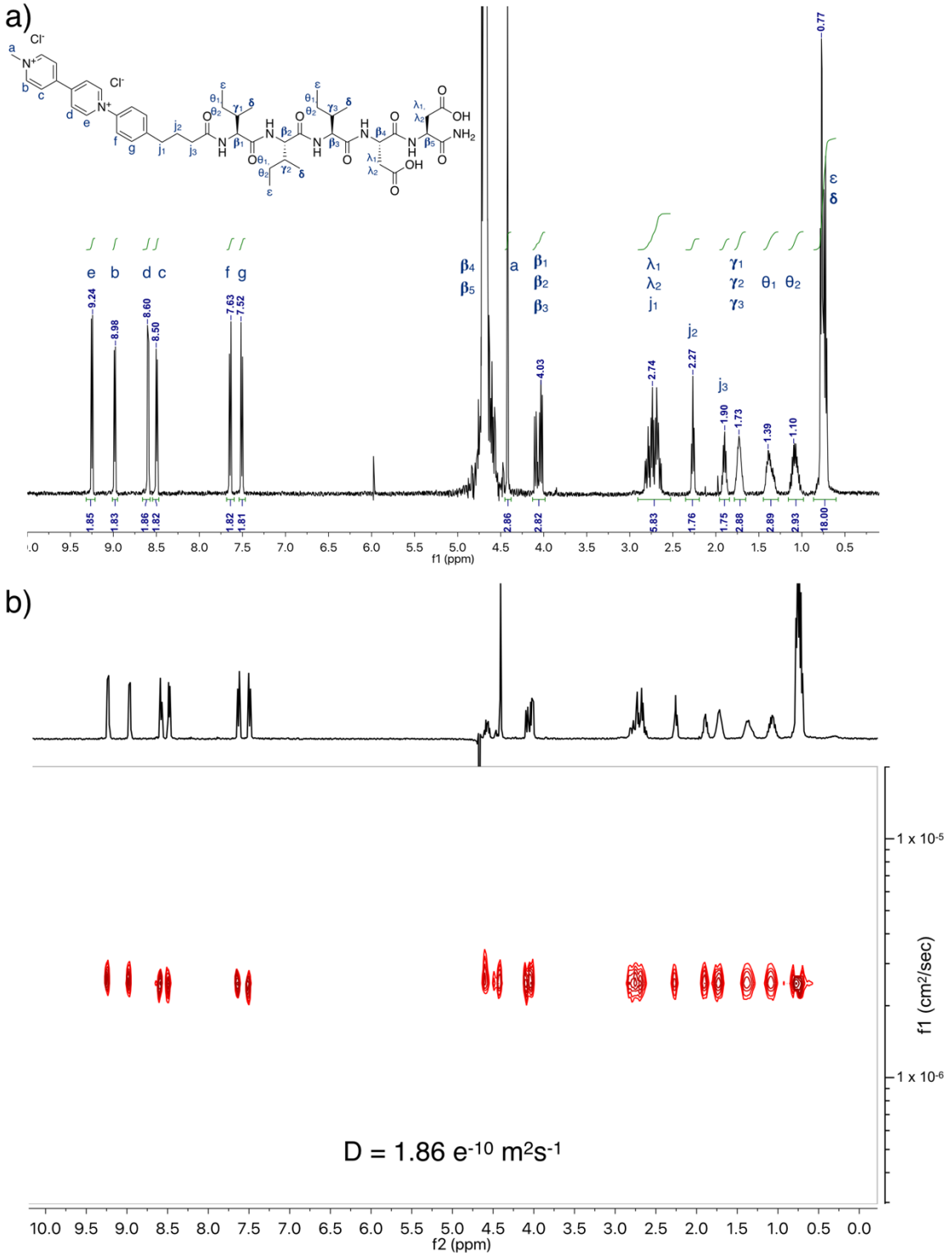

Figure S10. a) ^{1}H-NMR and b) DOSY spectra of AVI3D2 (500 MHz, D_2O).

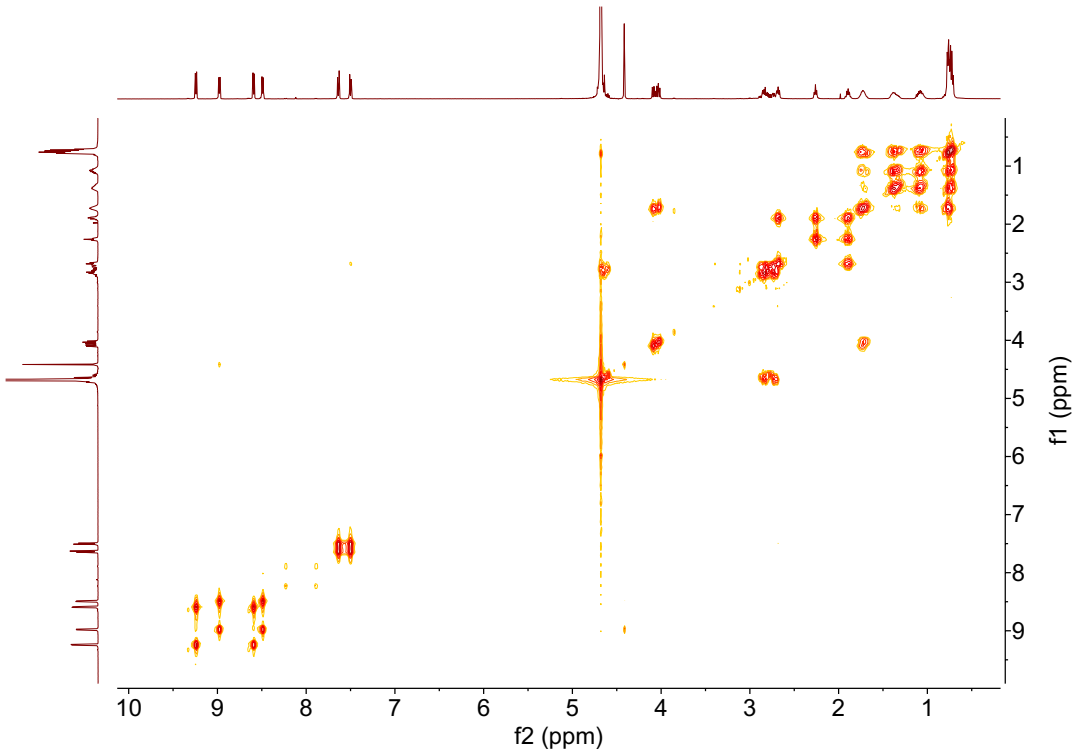

Figure S11.COSY spectra of AVI3D2 (500 MHz, D_2O).

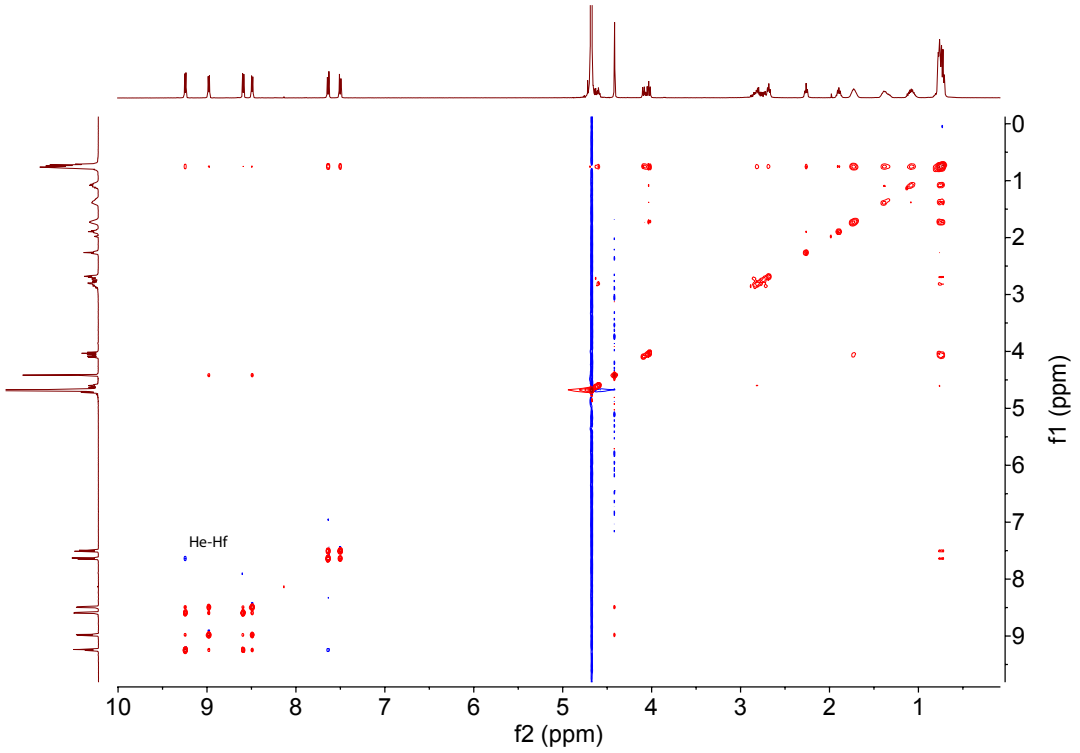

Figure S12. NOESY spectra of AVI3D2, pD 7.40 (500 MHz, D_2O).

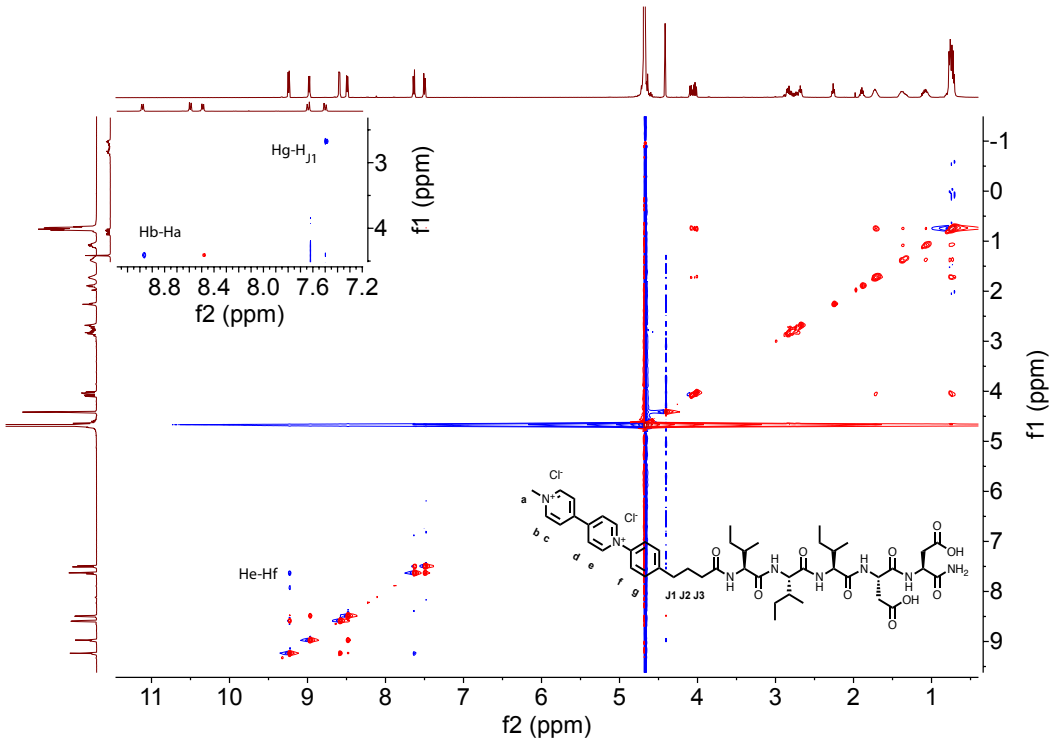

Figure S13. NOESY spectra of AVI3D2, pD 4.0 (500 MHz, D_2O/DCl).

Supplementary Discussion - NOESY 2D-NMR

The interactions between the AV moeities in AVI3D2 were investigated through NOESY 2D-NMR studies (Figures S7-8 and S12-13). Off-diagonal and positive phase signals were observed for the aryl-viologen units in both the AV and AVI3D2 molecules at 8 mM and pD 4, which suggests that in both cases intermolecular interactions exist between the viologens. Through-space interactions were recognized between the Hb-Ha, He-Hf, and Hg-Hj$_1$ protons (Figure S13) and for AV, additional signals were present for the He-Hd and Hb-Hg environments (Figure S8). At a concentration of 8 mM, AV is almost saturated, which may induce uncontrolled stacking of the molecule and the NOE signals. Combining these observations with the opposing behavior in PL spectra at similar conditions, the decrease in PL intensity of AVI3D2 provides evidence that the intermolecular interactions permit PET between stacked units. These 2D-NMR results confirmed our hypothesis that the AV region of the AVI3D2 can be brought into close contact via β-sheet interactions. Therefore, both the NOESY and fluorescence spectra of AVI3D2 suggest that pH can be used to trigger the β-sheet assembly of the peptide and in turn bring the AV units into close proximity via hydrophobic/π- π stacking.

UV-Vis and Fluorescence Measurements

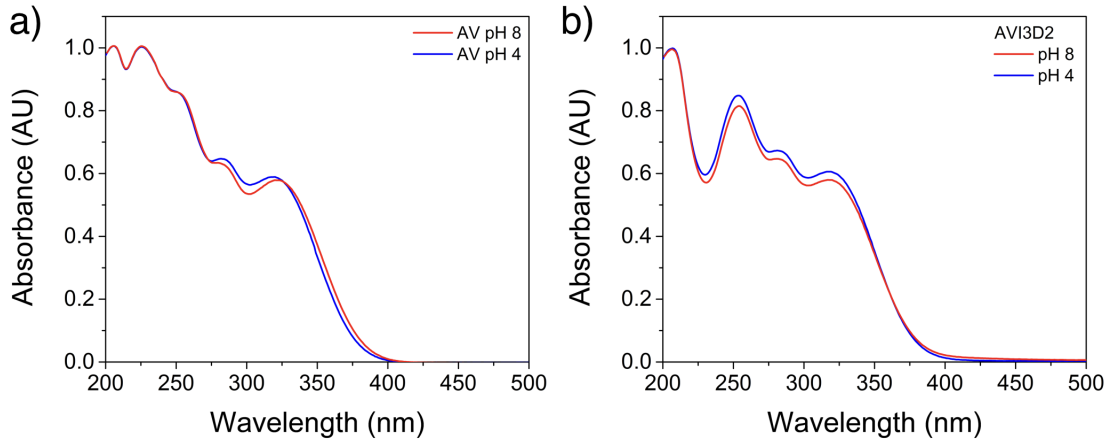

Figure S14. UV-Vis spectra of a) AV and b) AVI3D2 at different pH, all measurements were carried out at a concentration of 0.1 mM.

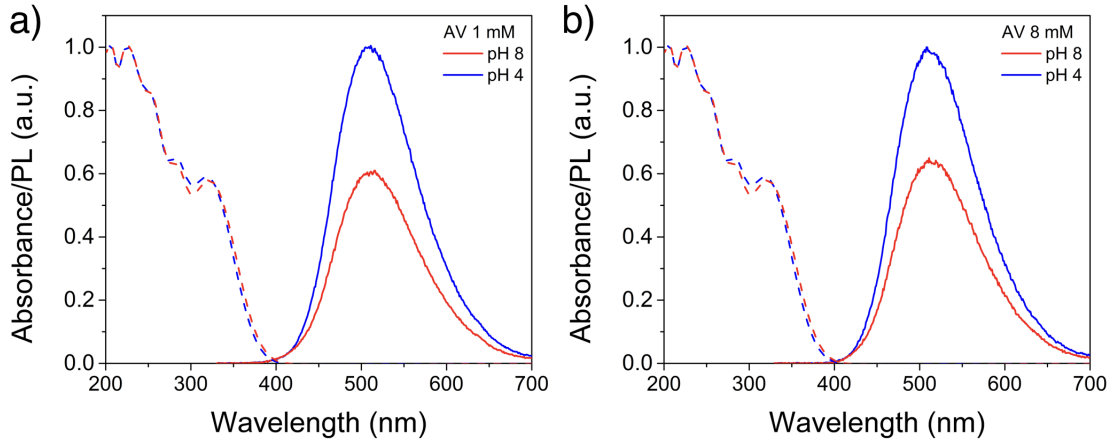

Figure S15. Normalized steady-state photoluminescence spectra of AV at different pH after excitation at 320 nm, a) 1 mM and b) 8 mM. Dotted lines represent absorbance of AV (0.1 mM) at the corresponding pH.

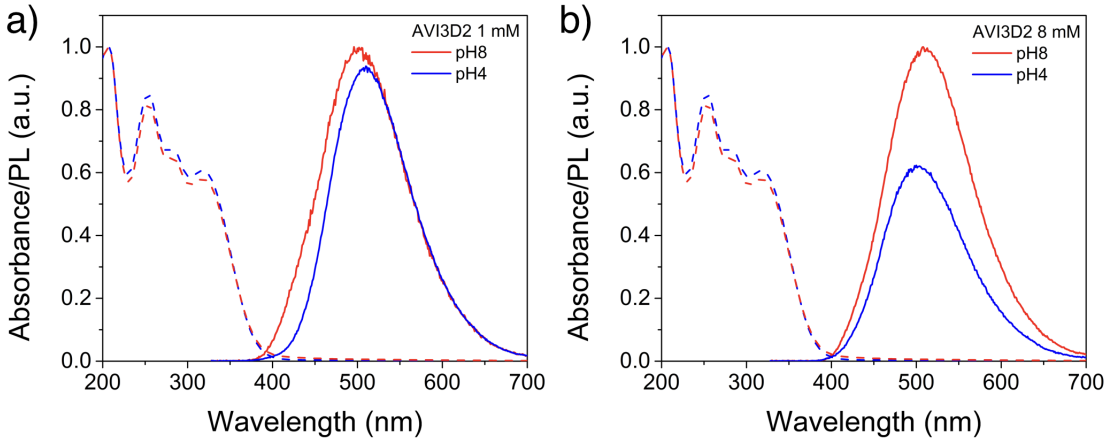

Figure S16. Normalized steady-state photoluminescence spectra of AVI3D2 at different pH after excitation at 320 nm, a) 1 mM and b) 8 mM. Dotted lines represent absorbance of AVI3D2 (0.1 mM) at the corresponding pH.

CD

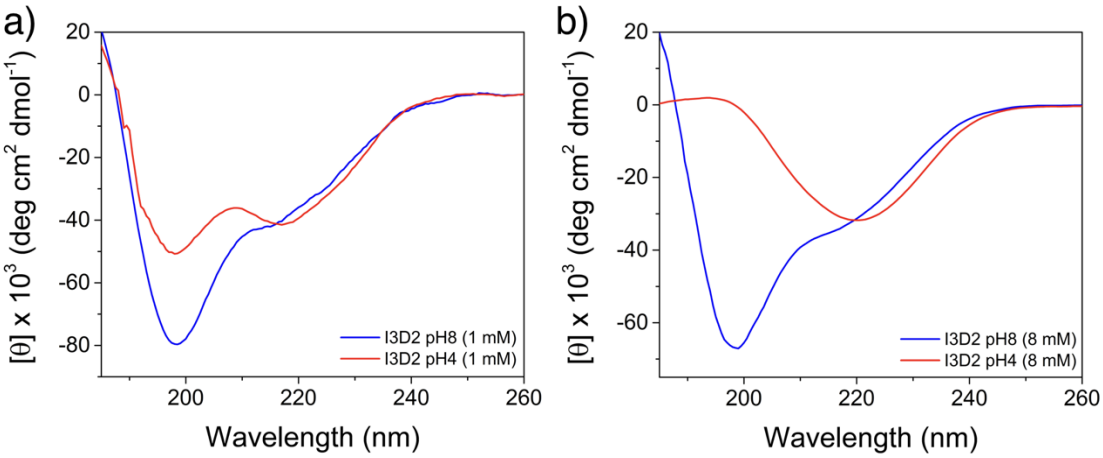

Figure S17. Circular Dichroism spectra of I3D2 peptide at different pH. a) 1 mM and b) 8 mM.

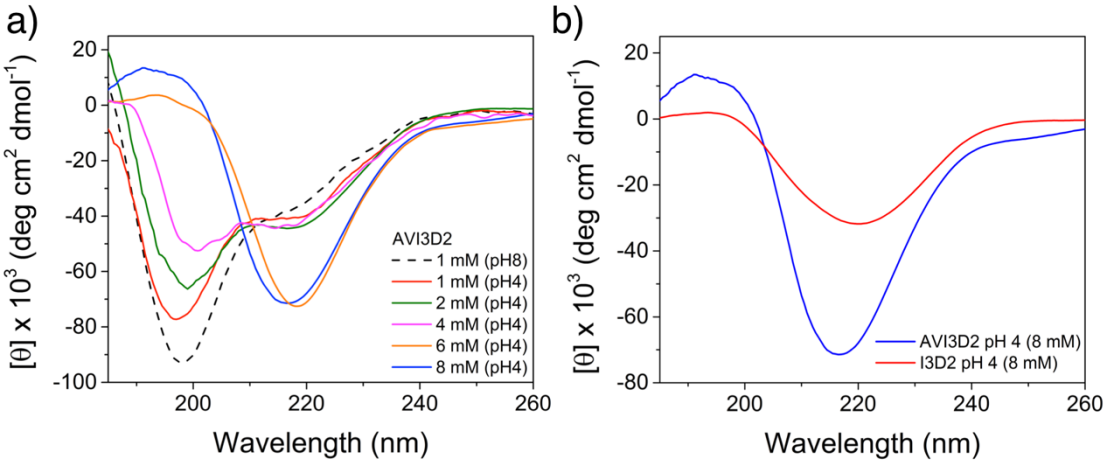

Figure S18. a) Circular Dichroism spectra of AVI3D2 at different concentrations and pH. b) Circular Dichroism spectra of AVI3D2 and the I3D2 peptide at a concentration of 8 mM and pH4.

FTIR

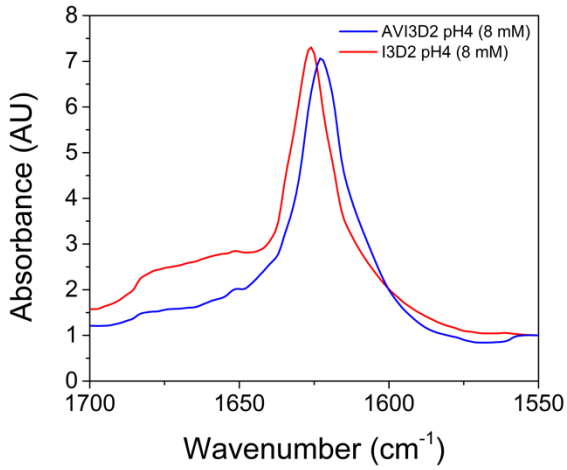

Figure S19. FTIR spectra of AVI3D2 and I3D2 peptide at a concentration of 8 mM and pH 4.

c-AFM

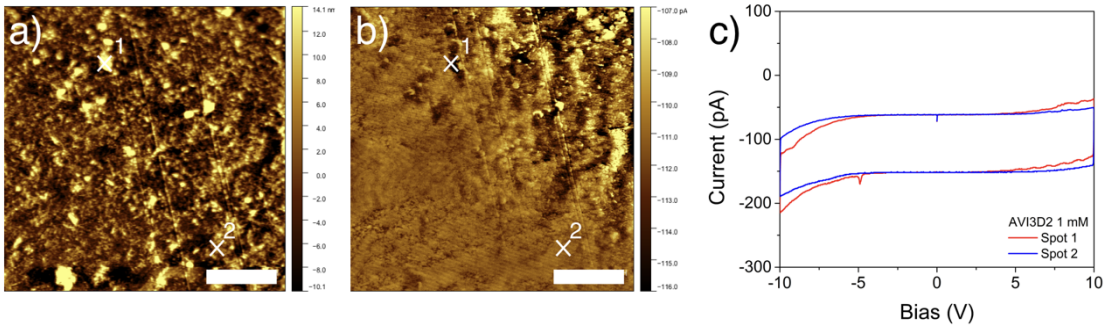

Figure 20. c-AFM of AVI3D2 (1 mM). a) Topography map, b) short-circuit current map and c) conductivity curves corresponding to spots 1 and 2. Scale bar on all the images is 5 μm.

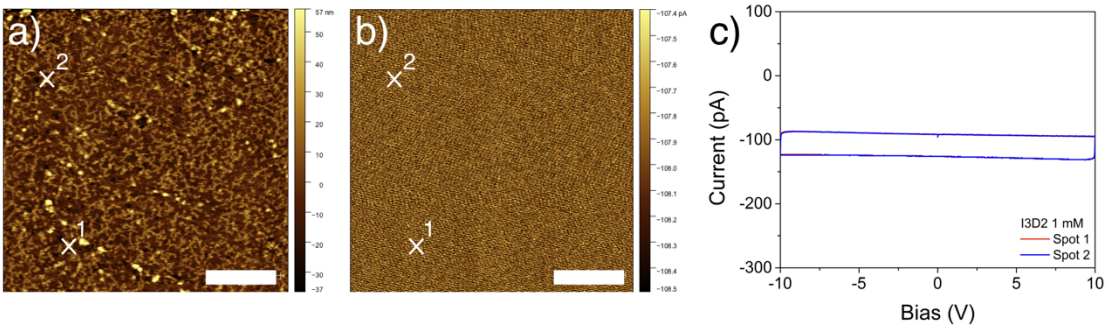

Figure S21. c-AFM of I3D2 (1 mM). a) Topography map, b) short-circuit current map and c) conductivity curves corresponding to spots 1 and 2. Scale bar on all the images is 5 μm.

ESR

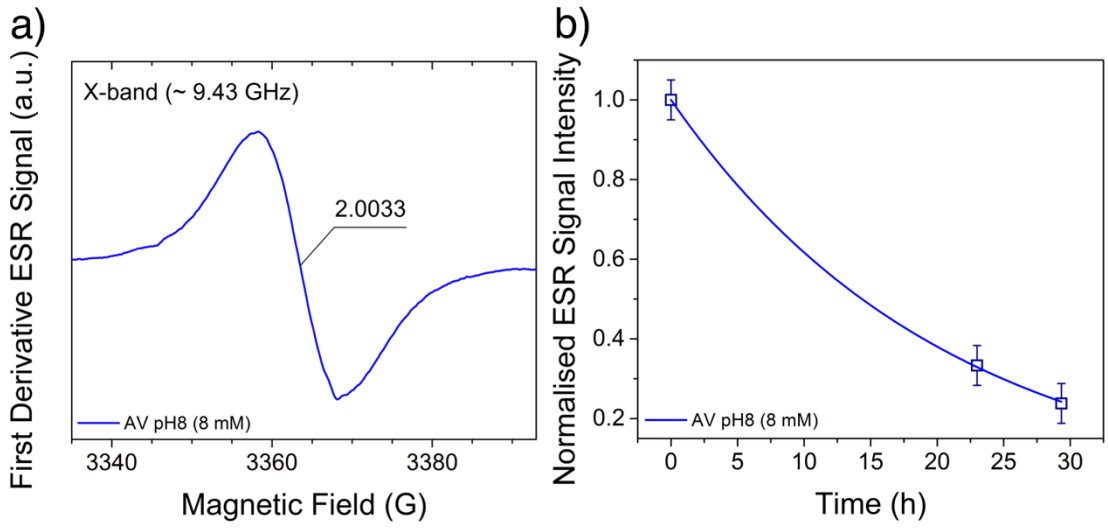

Figure S22. a) X-band (~ 9.43 GHz) first derivative ESR spectra of AV (8 mM) at pH8, the signal at g = 2.0033 ± 0.0002 originates from the viologen radical cations (spin concentration = 1.4 ± 0.1 x 10^{16} cm^{-3} and signal linewidth, ΔB_{pp} = 10.5 ± 0.2 G) following UV excitation. b) Radical signal decay curve following termination of UV irradiation (time constant = ~ 20 h).

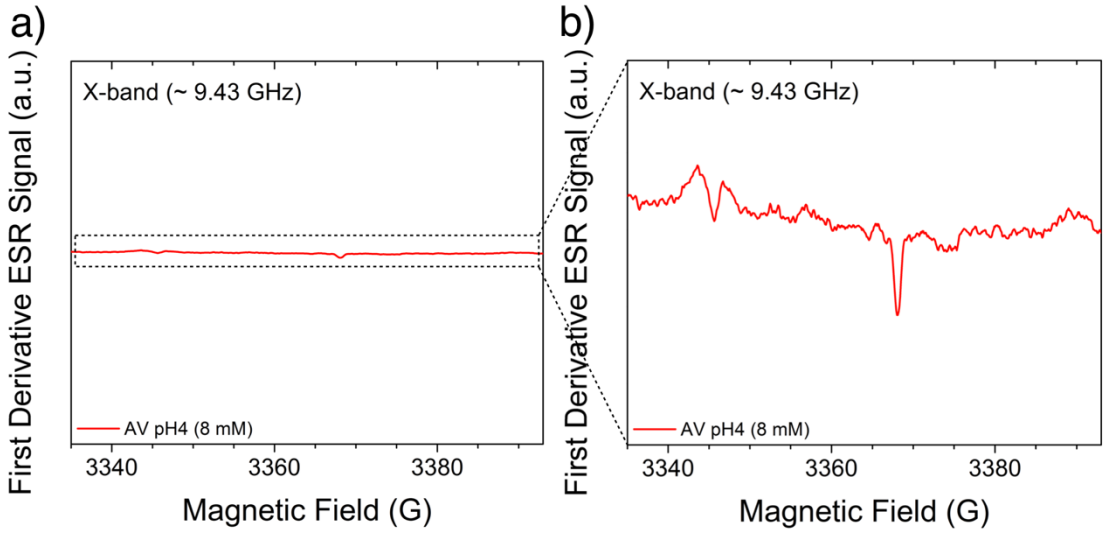

Figure S23. a) X-band (~ 9.43 GHz) first derivative ESR spectra of AV (8 mM) at pH4 and magnification of highlighted region demonstrating diamagnetic behavior (b).

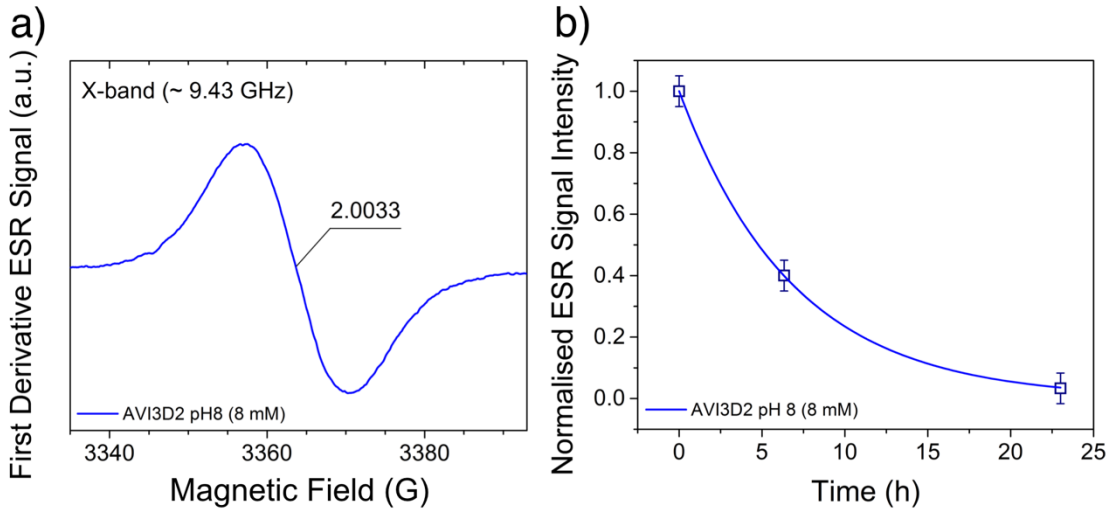

Figure S24. a) X-band (~ 9.43 GHz) first derivative ESR spectra of AVI3D2 (8 mM) at pH8, the signal at g = 2.0033 ± 0.0002 originates from viologen radical cations (spin concentration = 1.5 ± 0.1 x 10^{16} cm^{-3} and signal linewidth, ΔB_{pp} = 13.3 ± 0.2 G) following UV excitation. b) Radical signal decay curve following termination of UV irradiation (time constant = ~ 7 h).

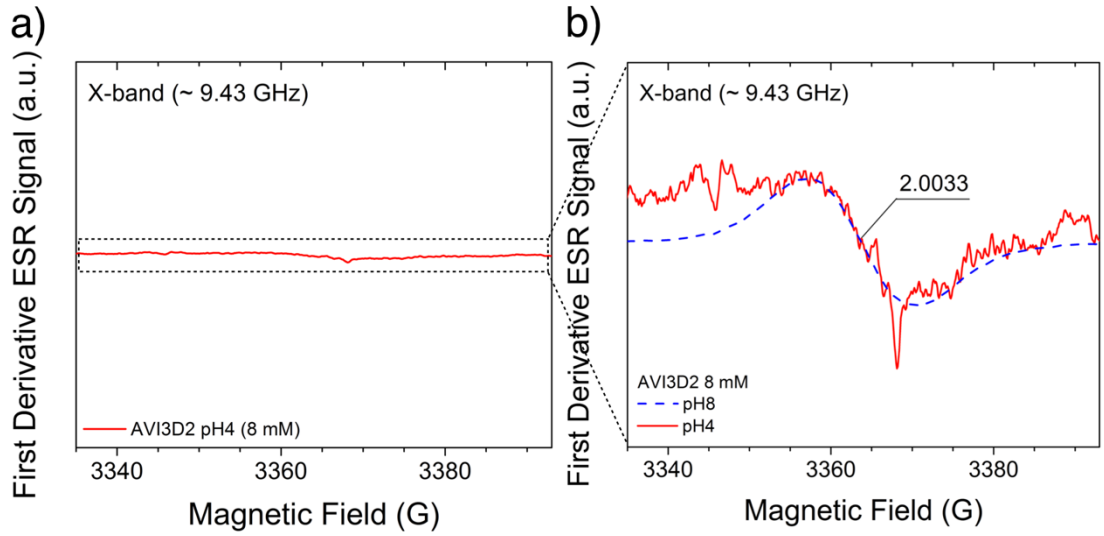

Figure S25. a) X-band (~ 9.43 GHz) first derivative ESR spectra of AVI3D2 (8 mM) at pH4. b) Magnification of highlighted region coupled with a rescaled AVI3D2 (8 mM) pH8 ESR signal overlay (dashed blue line). The weak ESR signal at g = 2.0033 ± 0.0002 originates from viologen radical cations.

Reference

[1] D. L. Griscom, Phys. Rev. B 22, 4192 (1980).